JOURNAL OF MATERIALS SCIENCE **34** (1999) 3747–3753

Undercooling, liquid separation and solidification of Cu-Co alloys

M. B. ROBINSON, D. LI*
Space Sciences Laboratory, NASA/Marshall Space Flight Center, Huntsville, Alabama 35812
T. J. RATHZ, G. WILLIAMS
University of Alabama, Huntsville, Alabama 35899, USA
E-mail: Delin.Li@msfc.nasa.gov

Large undercooling can induce not only various solidification pathways, but also a precursor reaction, or liquid separation. This paper deals with the latter effect of undercooling using examples of the Cu-Co system which has a flattened liquidus. Bulk Cu-Co alloys (about 7 mm in diameter) at compositions ranging from 10 to 100 wt % Co were highly undercooled using a fluxing technique. Except for compositions above 90 wt % Co, liquid separation was directly observed as undercooling exceeded a critical value depending on the composition. It was also confirmed by a microstructural transition from dendrites to droplets above the critical undercooling. Finally, calculations of the metastable miscibility boundary were made to analyze the experimental results.

1. Introduction

Liquid-phase separation can occur within either a *stable* or *metastable* miscibility gap (MG). The former features an equilibrium phase diagram, while the latter lies beneath the liquidus curve. During the past few decades much research [1, 2] has been carried out on the stable immiscible alloys on earth, and in space as well. It means that not only experimental attempts were made to produce aligned fibrous or particle dispersed composites, but also theoretical studies were involved on liquid phase nucleation, growth, coarsening and coagulation mechanisms. However, the second type of miscibility gap, namely phase separation in an undercooled liquid, has not yet received widespread attention, perhaps because of some difficulties in precisely determining the subliquidus MG.

The tendency for the metastable liquid demixing can often be judged by an appearance of the phase boundary, in particular the slope and curvature of the liquidus. Equilibrium phase diagrams containing a smoothly sloping liquidus are likely candidates for occurrence of metastable liquid separation. Submerged liquid MG exists in a number of metallic alloys, besides classical glasses. The droplet-shaped microstructures in Al-Be [3] and Ag-Pb [4] alloys processed by laser surface remelting and drop tube respectively were interpreted to have resulted from the metastable MG. Recently in a metallic glass forming system of multi-components [5], liquid-phase decomposition was observed in a deeply undercooled state, which could lead to the formation of nanocrystals.

Several Cu-based binary alloys such as Cu-Co [6], Cu-Fe [7], Cu-Cr [8] and Cu-Nb [9], have long been of special interest because of their potential high performance and metastable liquid MG. The first report of liquid-phase separation for the former two systems came from Nakagawa [10] who noticed a discontinuous change in the magnetic susceptibilities. Since the samples were described to be obviously oxidized during heating and quenching [10], the possibility cannot be precluded that the liquid separation was initiated by oxygen impurities. This effect of oxygen has been verified in other Cu-based alloys [11]. Moreover, the earlier paper is limited to relatively low undercooling near the critical point of the MG. Recently, Munitz and Abbaschian [12–14] utilized drop tube, electron beam melting, and electromagnetic levitation with subsequent splat cooling to study the effects of undercooling and cooling rate on the microstructure of Cu-Co alloys. A metastable MG was proposed in light of both the composition analysis on quenched discs and sample release temperatures from the levitation coil. However, in the drop tube experiments, no spherical samples were obtained [12]. For the latter two methods, there is electron beam or electromagnetic stirring in melts, giving rise to swirled droplets [13, 14]. Also it is difficult to understand that no droplet-like structure could be identified in some compositions. For instance, only dendritic structure was produced for the Cu-50 wt % Co alloy, even if it was undercooled far below their proposed MG [13, 14]. A more recent paper by Yamauchi *et al.* [15] reported some different results based on thermal analysis. They determined a separation temperature for $Cu_{50}Co_{50}$ which was 30 K less than that of Nakagawa [10]. Moreover Yamauchi claimed that the upper layer was Co-rich, while the lower part was Cu-rich. This

* NASA NRC Resident Research Associate.

separation tendency is in contrast to the observations of Nakagawa. Interpretations for the conflicting information were not available. Another point to note is that the metastable liquid separation was also indicated in the microstructure of melt-spun Cu-Co ribbons [16] where the undercooling was promoted by a high cooling rate.

Whether metastable melt separation can come into being depends mainly on the level of undercooling for a given system. As is well known, high undercooling in drops can be achieved by a variety of melt processing methods which are basically divided into two types: containerless [17] and fluxing [18]. The former includes electromagnetic or electrostatic levitation, drop tube and atomization. In the first case the levitation force, especially in an electromagnetic field, usually gives rise to strong perturbations in molten drops and makes the occurrence of liquid separation hardly detectable. In fluxing techniques, the melt is isolated from the solid container and cleaned by an appropriate slag glass. Studies show that comparably large undercoolings of bulk samples, for example, hypercooling [19] in completely miscible Co-Pd alloys, have been claimed using the fluxing method. In addition, the samples can be quite stationary during cooling, which may afford new opportunities for directly measuring liquid phase separation prior to solid phase growth. The objective of this study is to employ a fluxing technique to investigate undercooling, liquid separation and solidification of Cu-Co alloys in the following aspects: experimental determination and thermodynamic modeling of the metastable MG, microstructural selection upon undercooling, and effects of undercooling and composition on droplet coarsening.

2. Experimental

High purity copper shots (99.9999%) and cobalt pieces (99.998%), together with about 0.3 g flux agents (a Duran glass) were inserted into an Al_2O_3 crucible for *in situ* alloying and denucleating Cu-Co samples. Each sample had a mass of 1.3 g. The crucible was placed in a RF (radio frequency) coil. Under an ultrahigh vacuum (pressure $\leq 1.3 \times 10^{-5}$ Pa), the sample was preheated to 1300 K for 15 min to dehydrate the flux and evaporate other surface impurities. It was observed that there was a definite relation between the in *vacuo* treatment and the attainment of major undercoolings. After the in *vacuo* treatment, the chamber was back-filled with He-6%H_2 gas (purity better than 5N) to 78 kPa. And then the sample was subjected to a number of successive heating-cooling cycles. In order to avoid electromagnetic effect, the RF power was switched off when the melt started to cool. At least three samples were run for a given composition. A single color pyrometer (Mikron, model 190 with a resolution of 0.1 K) was used for temperature measurement. Temperatures were calibrated with the peritectic solidification at 1385 K and the liquidus temperature. By repeated microsectioning of the epoxy-mounted samples, the largest droplet diameter was measured with optical microscopy. The samples were also examined using electron microprobe for WDS (wavelength dispersive spectroscopy) quantitative analysis.

3. Results and discussion

3.1. Metastable liquid separation

The total mass loss of a processed sample was less than 0.7%, and the microprobe analysis shows that little has changed in the bulk compositions for specimens. Fig. 1 illustrates the measured cooling profiles of three Cu-70 wt % Co samples and one Cu-90 wt % Co sample with different undercoolings. All the curves show relatively low cooling rates of 50 to 70 K/s before solid nucleation, but they differ in the undercooling behavior. The liquidus temperature, T_L, can be determined from the first thermal arrest on the curve (a) of a sample with very small undercooling. The measured T_L is identical to value on the equilibrium phase diagram [20], which verifies the present temperature calibration. For curve (b), the melt was smoothly undercooled 130 K below the T_L and then led to a recalescence corresponding to the growth of primary Co dendrites. Also for all cases, after further cooling, the peritectic transformation can be seen at T_P (at about 1385 K). At still deeper undercooling, additional anomalies appear prior to the major recalescence, as marked by T_S in Fig. 1c. This unusual phenomenon neither emerged at small undercooling, nor arose from the flux agent of which the glass transition temperature is lower than 800 K. The anomalous point was observed in a wide range of compositions from 10 to 80 wt % Co, when they were highly undercooled. However the Cu-90 wt % Co alloy (Fig. 1d) exhibited a continuous cooling profile without any temperature inflection prior to solid nucleation, even if it was undercooled more than curve (c). The reason is that the 90 wt % Co composition is located in the area of single Co phase. Therefore, it can be inferred that the anomalous behavior in Fig. 1c can be attributed to a precursor reaction, namely a phase

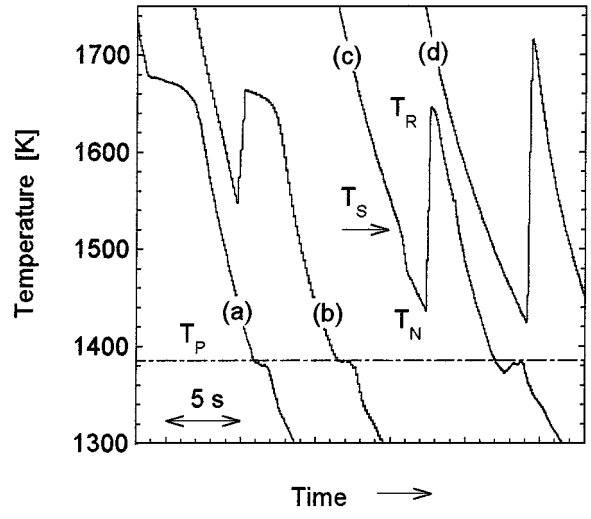

Figure 1 Measured cooling curves for three Cu-70 wt % Co samples: (a) little ΔT, (b) $\Delta T = 130$ K and (c) $\Delta T = 245$ K, and one Cu-90 wt % Co sample (d) $\Delta T = 310$ K. T_P, T_N, T_S, and T_R are peritectic, solid nucleation, liquid separation, and maximum recalescence temperature, respectively.

separation in the sufficiently undercooled melts. The first angular point on the cooling curve prior to recalescence onset is referred to hereafter as T_S, the temperature at which separation into two liquid phases L1 (more Co content) and L2 (more Cu content) begins. Note that two types of T_S arrests were observed: convex arrest like Fig. 1c for compositions from 70 to 80 wt % Co, and concave one for compositions below 70 wt % Co. Therefore, whether the liquid separation is endothermic or exothermic cannot be determined by the shape of the T_S arrest alone (Differential Thermal Analysis is needed). It may be also caused by a wetting behavior change with different compositions during liquid separation. However, the arrest shape is not a critical concern in this investigation, rather than determination of the T_S point is important. After separation at T_S, the system was able to be further undercooled until a solid nucleation temperature, T_N, as shown in Fig. 1c. As yet there has been no liquid undercooled below the Curie temperature in this study. The separation temperature T_S is strongly dependent upon the alloy composition, while the T_N is a weak function of composition despite an increase in the maximum undercooling achievable with the Co content. The weak relation between T_N and composition has a bearing upon the near-horizontal appearance of the liquidus in this system. The duration time from T_S to T_N, termed Δt, plays an important role in the growth of liquid droplets.

By plotting the measured T_S of twelve different compositions on the phase diagram [20], the metastable liquid miscibility boundary has been established and is presented in Fig. 2. By comparison, our directly-determined gap is basically consistent with the previous MG which was derived from composition analysis on the quenched samples [14], however the present dome is depressed about 40 K. In Ref. [14], the drop release

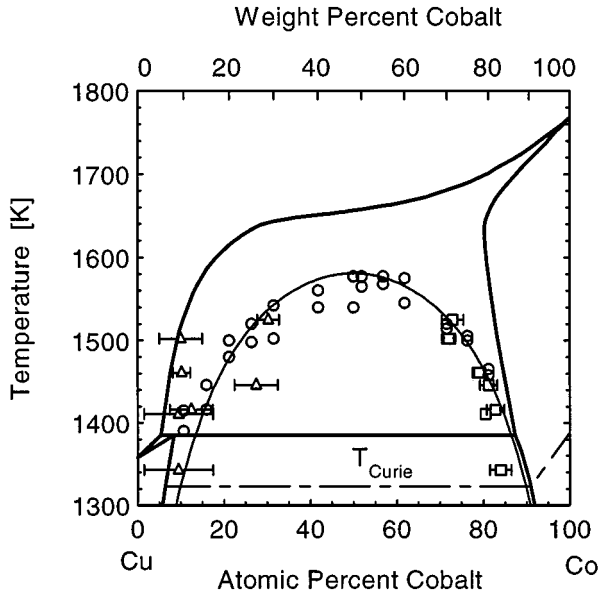

Figure 2 The phase diagram of Cu-Co [20] from liquid to 1300 K. Superposed on this diagram are: direct measurements of liquid separation (circles), calculated metastable miscibility dome (thin solid line), and droplet (squares) and matrix (triangles) compositions of seven Cu-30 wt % Co samples solidified at various undercoolings. T_{Curie} is the magnetic transformation temperature.

TABLE I Average compositions of droplet and matrix for seven Cu-30 wt % Co samples

Undercooling ΔT(K)	Atomic percent cobalt	
	Droplet	Matrix
116	72.9	30.3
139	72.0	10.0
180	79.0	10.2
195	81.2	27.5
225	82.8	12.4
230	80.5	9.5
298	84.0	9.5

temperature was taken as the actual solidification temperature, probably leading to an overestimate of the latter. After separation of a homogeneous melt at T_S, the compositions of the two liquids would be expected to follow the limits of the miscibility boundary during slow cooling. As such, it should be possible to construct the metastable MG postmortem by virtue of measured compositions and solidification temperature. However, difficulties arises in precisely determining the matrix composition. Taking examples of seven Cu-30 wt % Co specimens, Table I lists the average composition of droplets and matrices given by WDS, and undercooling. The concentration data represent the assessed results of several measurements. Superimposed on Fig. 2, the content points of well-defined droplets almost fall upon the miscibility boundary (small squares in Fig. 2), while the matrix data (small triangles) appreciably diverge from the dome. This suggests, with a view to setting up a metastable MG, that the composition analysis should focus on the well-defined droplets (see following section about microstructure), instead of the matrix. This is because the Co content in a solidified matrix is not uniform.

3.2. Microstructural selection

The amount of liquid undercooling ΔT is recognized as an essential parameter in determining the final solidified microstructures. As ΔT increased, all samples examined at compositions ranging from 10 to 80 wt % Co yielded two types of microstructures: dendritic, or droplet-shaped morphology. This composition range for separation is broader than that of a recent paper [13] where no liquid separation was observed for the Cu-50 and 80 wt % Co alloys. It means that deeper undercooling can be accessed in fluxing method than other techniques for the Cu-Co system, owing to the avoidance of external field stirring. The microstructural transition can be elucidated by two Cu-50 wt % Co samples in Fig. 3. At undercooling less than 80 K, the liquid was situated in a "liquid + solid" region of the phase diagram, so that solidification commenced in a normal way with the growth of primary α-Co dendrites (dark phase in Fig. 3a). The Cu phase (bright) was formed through the peritectic reaction. The whole sample was full of this dendritic morphology. Once undercooled below T_S, liquid-phase separation happened and thus resulted in a microstructure in the form of droplets for one phase

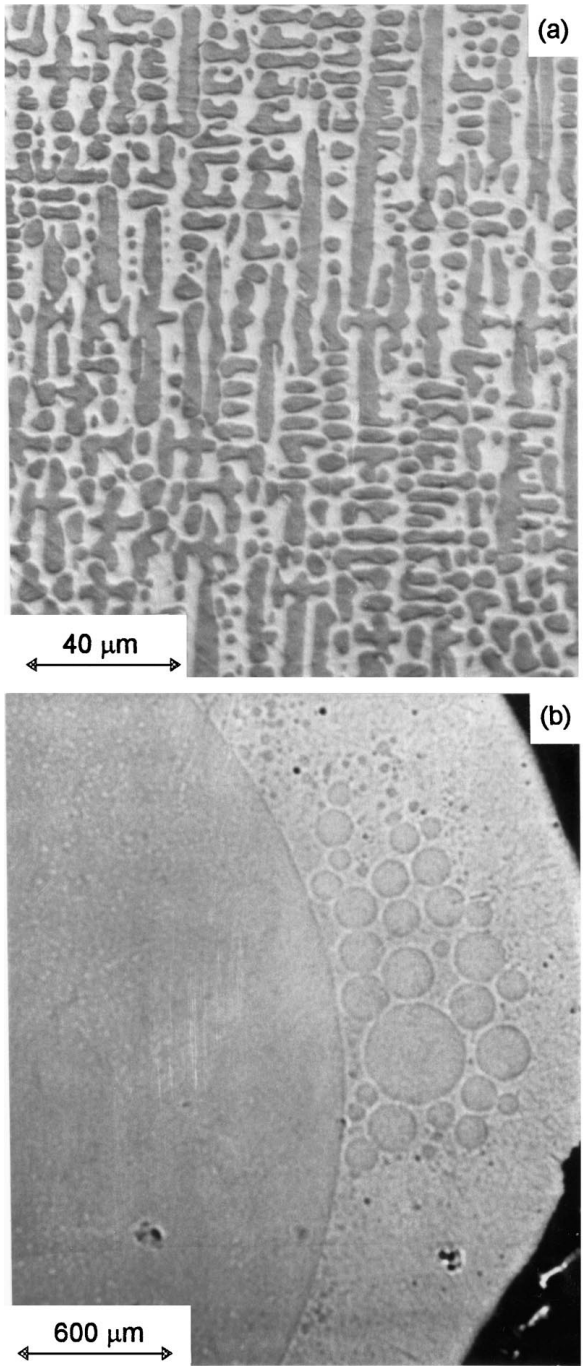

Figure 3 Microstructure transition from dendrites to droplets in the Cu-50 wt % Co alloy with the increase of undercooling: (a) $\Delta T = 20$ K, no separation; and (b) $\Delta T = 260$ K, indicating liquid separation.

throughout a matrix of another phase. Fig. 3b illustrates the separated interface between a large primary Co-rich droplet (left) and Cu-rich matrix for a Cu-50 wt % Co sample undercooled by 260 K. It was also observed that the big Co-rich droplet was suspended almost at the center of the sample, which is in contrast to the Co-rich phase located at the bottom [10] or top [15]. This discrepancy may be due to the different sample diameters ranging from 4 to 22 mm among these studies. It is known that the fluid flow velocity of a simple natural convection roll is dependent on the Grashof number, which is in turn proportional to the cubic of the sample size. Furthermore, microstructures with multiphase separation could notably be distinguished. Tiny Cu-rich droplets (bright) resulting from a secondary separation could be discerned inside the large Co-rich droplet, whereas the primary Cu-rich liquid was further decomposed into relatively small Co droplets. Phenomenon of multiphase separation has been well documented in glasses [21], but it has been rarely observed in stable metallic immiscibles. Since liquid metals possess a low viscosity and high diffusion coefficient, less time is needed to adjust the composition of the primary phases. However within a metastable MG of salient non-equilibrium features, the viscosity rises and diffusion coefficient declines with enhancing undercooling. In this case, complete diffusion was absent and multiphase separation in liquid became more likely to occur, especially for the alloys from 30 to 60 wt % Co.

Another factor influencing the final structure is a possible remixing owing to recalescence. Its maximum temperature T_R (see Fig. 1) was found to be dependent on the content of Co. The droplet-shaped structure could be completely retained in the Cu-rich alloys, since the T_R was lower than the miscibility gap T_S; while for the Co-rich alloys the growth of Co dendrites in large quantities during recalescence caused the T_R to go beyond the T_S, the system would be possibly in a miscible state again. However, it is noted that the temperature descended from the T_R to T_S within two seconds estimated from Fig. 1. It implies that a massive remixing might be kinetically difficult during this short period, thus keeping the droplet-shaped microstructures.

Once separated, the two liquids have different undercoolings with regard to their respective liquidus temperature. On the basis of Fig. 2, one can determine the amount of undercooling of Co-rich liquid L1 is larger than that of Cu-rich liquid L2, regardless of the absolute or reduced undercooling. As a result, L1 could solidify first according to the nucleation thermodynamics, whether or not it acted as droplet phase. Evidence for this solidification sequence is provided by micrographs in Fig. 4. For the Cu-30 wt % Co alloy, some dendrites within the matrix appeared to grow from the periphery of Co-rich droplets which had already solidified, as seen in Fig. 4a. For the Cu-60 wt % Co alloy there was a clearly opposite trend as displayed in Fig. 4b: inward growth of Co dendrites within Cu-rich droplets was preceded by solidification of the matrix. However, in view of the thermal behavior, only one major recalescence event was detected, as shown in Fig. 1c, which means solidification (forming α-Co phase) of L1 and L2 proceeded in a very quick succession. Since the two liquids were highly undercooled in one system, growth of one was prone to stimulate another.

3.3. Effects of undercooling and composition on droplet size

Since the system still remained a complete liquid during the period Δt between the separation T_S and solidification T_N, the liquid droplets could grow and move relative to the matrix and to each other. This incurs coarsening and coagulation of droplets, thus eventuating in a size distribution of the particles in solidified samples. Fig. 5 can serve to demonstrate the coarsening and

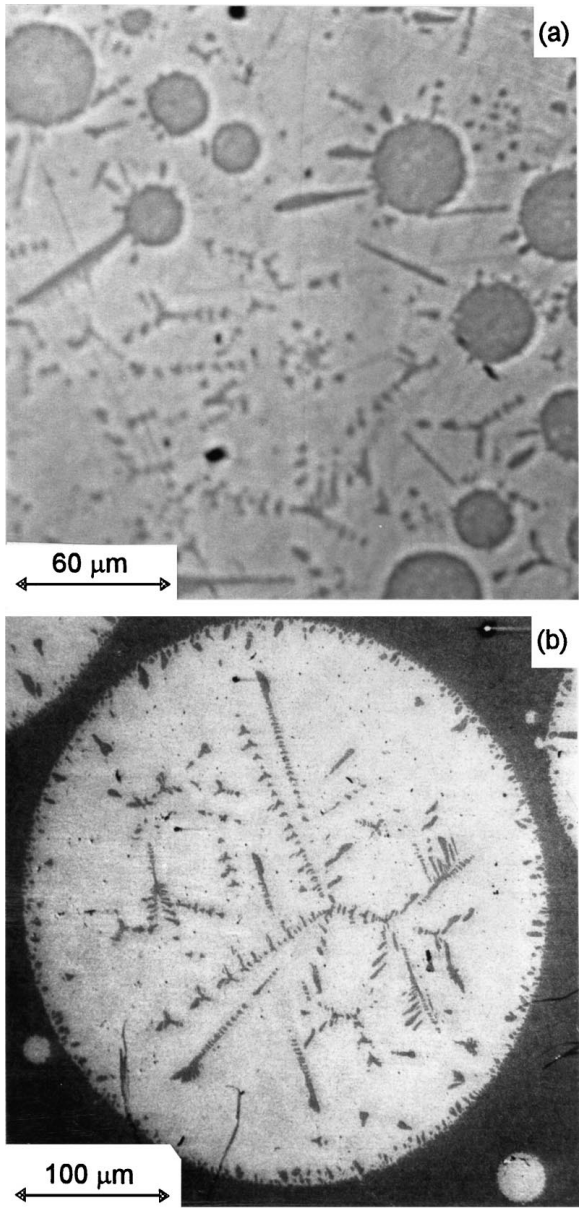

Figure 4 Hints of solidification sequence: (a) Co-rich droplets solidified first in the Cu-30 wt % Co alloy, and (b) Cu-rich droplets froze after the matrix for the Cu-60 wt % Co alloy.

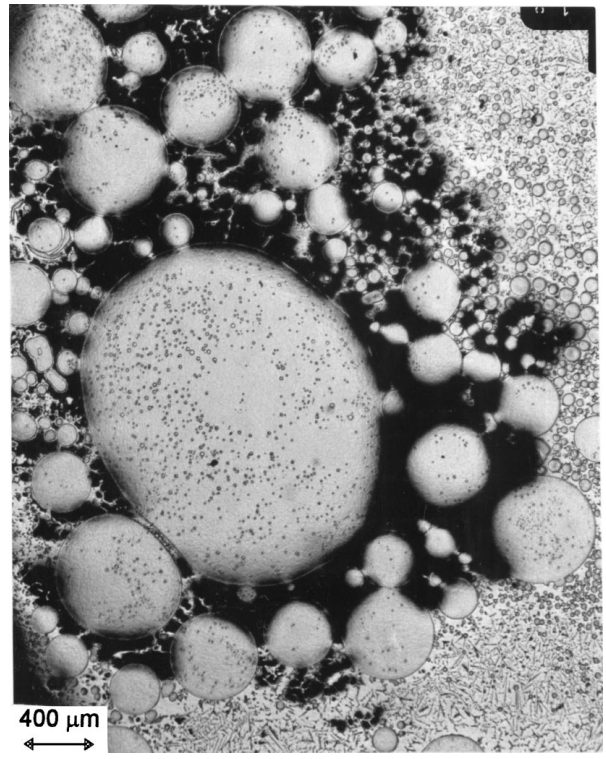

Figure 5 Coagulation of droplets in a Cu-30 wt % Co sample ($\Delta T =$ 210 K) which exhibits three different spherical regions.

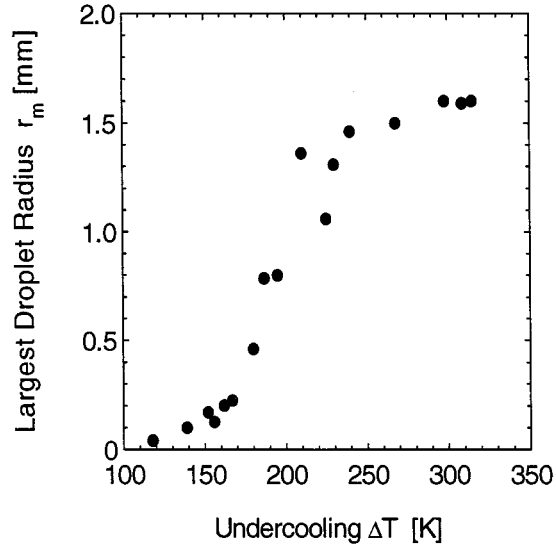

Figure 6 Relationship between the undercooling ΔT and biggest observed radius r_m of Co-rich droplets for the Cu-30 wt % Co alloy.

coagulation of liquid droplets. This figure shows a Cu-30 wt % Co sample undercooled by 210 K. It is seen that the large droplets could grow by absorbing smaller ones via a transfer of matter. Furthermore, some droplets collided with each other so that they may mutually lose surface energy by joining to form a single one. This micrograph highlights the main coalescence mechanisms in liquid-liquid mixtures. The solidified sample contained three regions of different droplet radius: about 40 μm, 300 μm, and 1 mm (the biggest one in this section), as illustrated in Fig. 5. The largest droplet radius observable, r_m could be chosen as a parameter to quantify the extent of coarsening [22]. The r_m was found in this study to be governed by both undercooling and composition which are discussed as follows.

Large undercooling usually leads to the refinement of microstructures, while an opposite tendency occurs in liquid immiscible alloys. Fig. 6 depicts this coarsening tendency with undercooling ΔT, namely the relationship between the r_m and ΔT for the Cu-30 wt % Co alloy. Clearly, the droplet radius increases with ΔT, because the higher undercooling is, the longer the interval Δt from T_S to T_N is, namely a longer coarsening time. However, the ΔT-r_m relationship can be further divided into three regimes. Note that there was no separation for ΔT less than 104 K for the Cu-30 wt % alloy. When ΔT was between 104 and 170 K, the droplets exhibited a slow growth which can be fitted into a power law ($r_m \propto \Delta t^{1/3}$). When ΔT varied from 170 to 200 K, the droplets were increasingly stirred due to various forces such as Marangoni and Stokes motions and thus coalesced. A coalescence event in turn induces another

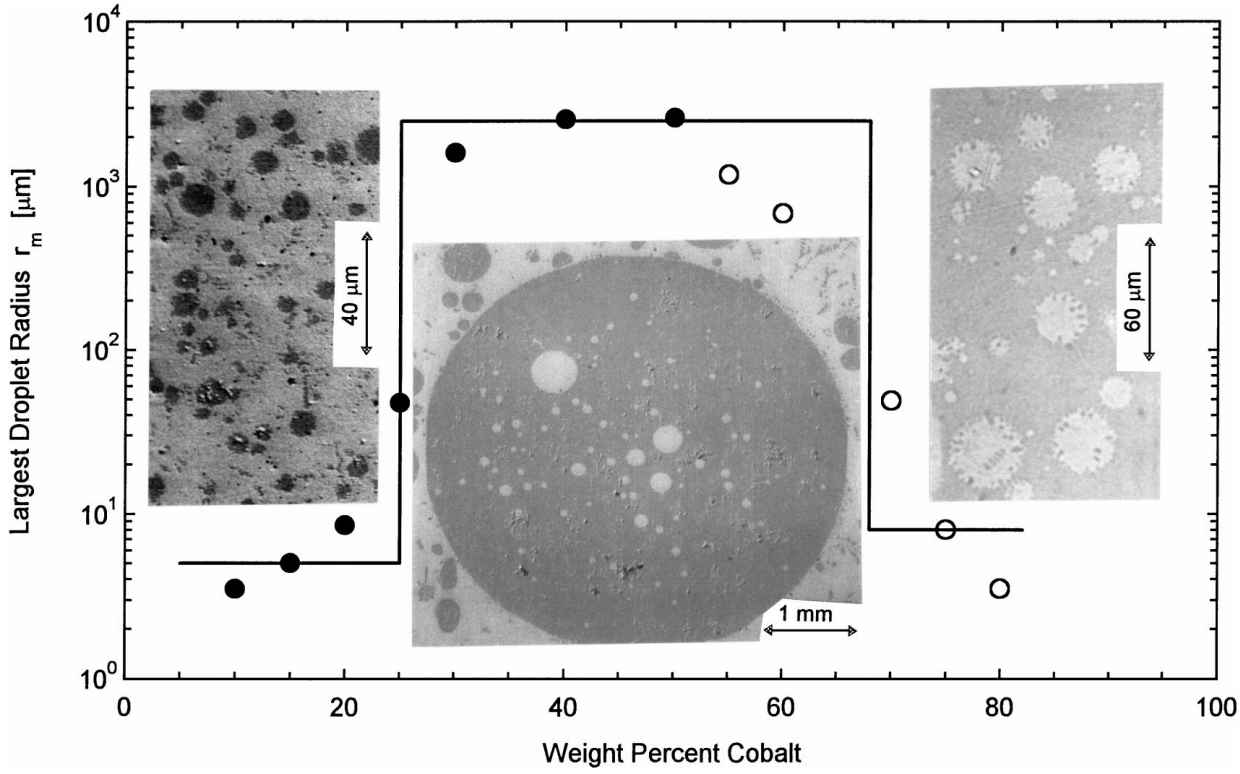

Figure 7 Maximum droplet radius observable r_m as a function of Co content. Solid and empty circles stand for Co-rich and Cu-rich droplets, respectively. Inset micrographs from the left to right correspond to a highly undercooled Cu-15, 40 and 70 wt % Co sample, separately.

coalescence, giving rise to a linear growth ($r_m \propto \Delta t$). For ΔT larger than 200 K, the radius r_m radius tended to a saturation value ($r_m \approx$ constant). As observed in fluid systems, the transition from $\Delta t^{1/3}$ at early times to δt^1 at late times was interpreted as a consequence of hydrodynamic effects [23], or coalescence [24].

Fig. 7 exposes a significant impact of composition on the largest droplet radius r_m. The data in this figure correspond to specimens of the highest undercooling attainable for each composition. Here one can reach the following results: Firstly, the radius r_m is less than 50 μm for the alloys at compositions below 20 or above 70 wt % Co. It is shown in the inset micrographs that a Cu-15 wt % Co specimen undercooled by 255 K formed with uniformly dispersed Co-rich spheres ($\leq$5 μm in radius) throughout the Cu matrix, and a Cu-70 wt % Co sample ($\Delta T = 228$ K) abounded with fine Cu-rich particles. This means that dispersed microstructures can be obtained on both sides of the metastable MG. However, for the stable immiscible alloys, fine droplets have been observed only on one side [1]. Secondly, the liquid droplets were coarsened seriously when the volume fraction of the minority component, v, is higher than 20%. This critical volume fraction is consistent with Walter's results [25] on silicate glass and stable immiscible alloys. It follows that the volume fraction of the minority component plays a vital part in liquid droplet coagulation. As a consequence, an eminently large droplet of up to 2.5 mm in radius was found, as shown in the middle micrograph of Fig. 7 for a Cu-40 wt % Co sample undercooled by 245 K. Inside this biggest Co-rich droplet, the small bright spheres (Cu-rich) resulted from multiphase separation. Thirdly, a functional change of phases occurred near the composition corresponding to the critical point. When the Co content is below 55 wt %, the Co-rich L1 appears as droplet phase (solid circles); while above 55 wt % Co, L1 takes over the matrix function and the Cu-rich L2 is turned into droplet phase (empty circles). It is understandable that the minority liquid-phase takes the form of droplets so as to diminish the interfacial energy in the system.

3.4. Calculations of the metastable MG

Recently, computer simulations [26] of phase decomposition for the Cu-Co system have been performed on the basis of the Onsager diffusion equation, in order to build a metastable binodal line. As described in Ref. [26], the consolute point of the calculated binodal touches the liquidus, indicating the critical undercooling for liquid decomposition approaches zero. Unfortunately, the actual Cu-Co system does not fall into this simulated picture, since the transformation sequence is that the stable solid phase is always solidified first from a homogeneous liquid undercooled slightly. Perepezko [27] has examined the thermodynamic conditions of metastable miscibility in terms of the relation for the slope of the liquidus for binary alloys, and formulated an equation to estimate the critical undercooling ΔT_c:

$$\Delta T_c = \frac{F_B + RT_c/2}{2RT_L}\left[-\frac{dT_L}{dx_A}\right]_{x_A=0.5} \quad (1)$$

where subscripts A and B correspond to component Cu and Co respectively, F is the heat of fusion, $F_B = 1.55 \times 10^4$ J/mol (Material properties required in this paper were taken from Ref. [28]), R is the gas constant, T_c is the consolute temperature of miscibility dome, and x is the atomic fraction. According to Equation 1,

the calculated ΔT_c being about 50 K is not deviated vastly from the experimental value of 80 K. Although Equation 1 directly relates the MG to the slope of the equilibrium liquidus, the whole boundary cannot be deduced. Hence a thermodynamic calculation is desirable. Using a regular solution model, the liquid Gibbs energies of mixing can be expressed as [29]:

$$\Delta G_L = \Omega(L) x_A x_B + RT(x_A \ln x_A + x_B \ln x_B) \quad (2)$$

where $\Omega(L)$, T_{mA} and T_{mB} denote the interaction parameter, melting point of Cu and Co, respectively. Thermodynamic evaluations of the equilibrium Cu-Co phase diagram have been made by Hasebe and Nishizawa [30]. They put forward a high positive value of interaction parameter in the system: $\Omega(L) = 1.75RT_{mB}$ and $\Omega(S) = 2.0RT_{mB}$. That is to say, the interaction parameter may accrue as the temperature goes down. For simplicity, in this paper, $\Omega(L)$ was treated as a function of temperature T in the range of T_P (1385) to 1700 K, and a constant beyond this T range in our calculation. Thus $\Omega(L)$ can be modified as:

$$\Omega(L) = [2 - 1.05 \times 10^{-3} \times (T - T_P)] \times RT_{mB} \quad (3)$$

The ΔG_L was calculated according to Equation 2. The curves of the energy versus composition clearly demonstrated a region of demixing over a certain undercooling level. Accordingly, the calculated metastable binodal was obtained through drawing a common tangent on the two negative humps of energy curves. With the exception of a few points, for example, for Cu-40 wt % Co, the modeling (thin solid line in Fig. 2) agrees well with measurements (empty circles).

4. Conclusions

A substantial degree of undercooling up to 330 K has been achieved for bulk Cu-Co alloys in a flux. It appears that the liquid undercoolability is limited by the liquid separation and Curie temperature in this system. For the first time, the metastable liquid MG has been directly established in a composition range from 10 to 80 wt % Co. There is good agreement between the calculated and measured metastable liquid MG.

By correlating the separation temperature and solidification temperature with resulting microstructures, the morphology development has been defined clearly. Upon solidification of the separated liquid after deep undercooling, droplet-shaped morphologies were formed for all alloys containing 10 to 80 wt % Co, though different droplet distributions were exhibited. For a given composition, the largest droplet radius increases with undercooling. Enhancing undercooling also resulted in the growth kinetics transition of droplets from a slow growth to fast growth and to saturation stage. More strikingly, the droplet size is influenced by the alloy composition. Uniformly dispersed microstructures were obtained on both sides of the metastable liquid MG; while the droplet size distribution for the alloys between 30 to 65 wt % Co contained a steep jump from small spheres to a prominently big one of 5 mm in diameter.

Acknowledgements

This work was performed while one of the authors (DL) held a National Research Council-(NASA MSFC) Research Associateship. The authors also thank G. Jerman for microprobe analysis, and D. M. Herlach and L. Ratke for valuable discussions.

References

1. See, for example, in Proceedings of an International Workshop on Immiscible Liquid Metals and Organics, Bad Honnef, May 1992, edited by L. Ratke (DMG Informationsgesellschaft mbH, Oberursel, 1993).
2. B. VINET and J. J. FAVIER, *Mater. Sci. Forum* **215/216** (1996) 271.
3. J. W. ELMER, M. J. AZIZ, L. E. TANNER, P. M. SMITH and M. A. WALL, *Acta Metall. Mater.* **42** (1994) 1065.
4. R. F. COCHRANE, P. V. EVANS and A. L. GREER, *Mater. Sci. Eng.* **98** (1988) 99.
5. S. SCHNEIDER, P. THIYAGARAJAN and W. L. JOHNSON, *Appl. Phys. Lett.* **68** (1996) 493.
6. T. NISHIZAWA and K. ISHIDA, *Bull. Alloy Phase Diagrams* **5** (1984) 161.
7. O. DROBOHLAV, W. J. FILHO and A. R. YAVARI, *Mater. Sci. Forum* **225–227** (1996) 359.
8. K. ZENG and M. HAMALAINEN, *Calphad* **19** (1995) 93.
9. T. W. ELLIS, I. E. ANDERSON, H. L. DOWNING and J. D. VERHOEVEN, *Metall. Trans.* **24A** (1993) 21.
10. Y. NAKAGAWA, *Acta Metall.* **6** (1958) 704.
11. J. D. VERHOEVEN and E. D. GIBSON, *J. Mater. Sci.* **13** (1978) 1576.
12. A. MUNITZ and G. J. ABBASCHIAN, *ibid.* **26** (1991) 6458.
13. *Idem., ibid.* **33** (1998) 3639. Note: there are four typographical errors in Table I.
14. A. MUNITZ and R. ABBASCHIAN, *Metall. Mater. Trans.* **27A** (1996) 4049.
15. I. YAMAUCHI, N. UENO, M. SHIMAOKA and I. OHNAKA, *J. Mater. Sci.* **33** (1998) 371.
16. X. SONG, S. W. MAHON, B. J. HICKEY, M. A. HOWSON and R. F. COCHRANE, *Mater. Sci. Forum* **225–227** (1996) 163.
17. T. J. RATHZ, M. B. ROBINSON, W. H. HOFMEISTER and R. J. BAYUZICK, *Rev. Sci. Instrum.* **61** (1990) 3846.
18. J. H. PEREPEZKO, *Mater. Sci. Eng.* **65** (1984) 125.
19. G. WILDE, G. P. GORLER and R. WILLNECKER, *Appl. Phys. Lett.* **69** (1996) 2995.
20. ASM's Binary Alloy Phase Diagrams on CD-ROM, 2nd ed. (ASM International, 1996).
21. W. VOGEL, "Glass Chemistry" (Spring-Verlag, Berlin, 1994) p. 92.
22. L. RATKE and S. DIEFENBACH, *Mater. Sci. Eng.* **R15** (1995) 263.
23. N. C. WONG and C. M. KNOBLER, *Phys. Rev. A.* **24** (1981) 3205.
24. D. BEYSENS, in "Materials and Fluids under Low Gravity," edited by L. Ratke, H. Walter and B. Feuerbacher (Springer-Verlag, Berlin, 1996) p. 4.
25. H. U. WALTER, in Proceedings of an RIT/ESA/SSC Workshop on the Effect of Gravity on the Solidification of Immiscible Alloys, Jarva Krog, January 1984, edited by H. Fredriksson (ESA SP-219, The Netherlands, 1984) p. 47.
26. T. KOYAMA, T. MIYAZAKI and A. MEBED, *Metall. Mater. Trans.* **26A** (1995) 2617.
27. J. H. PEREPEZKO, *Mater. Sci. Eng.* **A226–228** (1997) 374.
28. T. ILDA and R. I. L. GUTHRIE, "The Physical Properties of Liquid Metals" (Clarendon Press, Oxford, 1988).
29. R. W. CAHN and P. HAASEN, "Physical Metallurgy" (Elsevier Science BV, North-Holland, 1996) p. 471.
30. M. HASEBE and T. NISHIZAWA, *Calphad* **4** (1980) 83.

Received 10 February
and accepted 24 November 1998